

Supporting Information for

Boronic acid-mediated mucin/surface interactions of zwitterionic polymer brushes

Karla E. Cureno Hernandez¹, Jeonghun Lee¹, Sunghoon Kim¹, Zach Cartwright², Margarita Herrera-Alonso^{1,3}*

¹ School of Materials Science and Engineering, Colorado State University, Fort Collins, Colorado, 80523, United States

² School of Biomedical Engineering, Colorado State University, Fort Collins, Colorado, 80523, United States

³ Department of Chemical and Biological Engineering, Colorado State University, Fort Collins, Colorado, 80523, United States

*Email: m.herrera-alonso@colostate.edu

Table of contents

	Page
Fig. S1. Solution-polymerization of MPC using (3-trimethoxysilyl)propyl 2-bromo-2-methylpropionate as the initiator. (A) NMR data for final product after 18 h of reaction. (B) SEC of the free polymer in solution after 18 h in TFE. (C, D) Kinetic plots for the ARGET ATRP of MPC conducted under the same conditions as those reported in the manuscript, exhibiting the behavior characteristic of a controlled polymerization.	3
Fig. S2. High resolution XPS spectra of C _{1s} , N _{1s} , and P _{2p} peaks of –ATRP (top), –PMPC (middle) and –APBA (bottom) silicon wafers. The black dots represent experimental data and the solid gray line corresponds to the fitted data.	4
Fig. S3. High resolution XPS spectra of C _{1s} , N _{1s} , and P _{2p} peaks of –ATRP (top), –PMPC (middle) and –APBA (bottom) silica nanoparticles. The black dots represent experimental data and the solid gray line corresponds to the fitted data.	5
Table S1. Elemental surface composition of silica nanoparticles with different surface chemistries, obtained by XPS.	6
Fig. S4. Characterization of surface modified silica nanoparticles. (A) FTIR spectra of –Br (black), –PMPC (blue), and –APBA (red) samples showing characteristic vibrations of functional groups present in each. (B) Fluorescence emission spectra of –PMPC and –APBA samples demonstrating the appearance of a fluorescent species only after conjugation of ARS with the boronic acid.	7
Analysis of light scattering data	8
Fig S5. Hydrodynamic diameter and polydispersity of SiNP–PMPC samples at different mucin concentrations and pH values at a SA:EG ratio of 1:1. The solid horizontal dark gray line represents the original dimensions of the particles in DI water (i.e., prior to incubation).	9
Fig. S6. Dynamic light scattering data of SiNP–APBA samples for different sialic acid:end group (SA:EG) ratios, and at pH 3.0 (A, B), 5.4 (C, D), and 7.4 (F, G). The shape of the correlation functions confirm the unimodal distribution of their corresponding hydrodynamic diameter curves. Moreover, the slower decay of the correlation function observed at pH 3.0 with decreasing SA:EG ratio confirms an increasingly more favorable interaction between mucin and the nanoparticle surface.	10

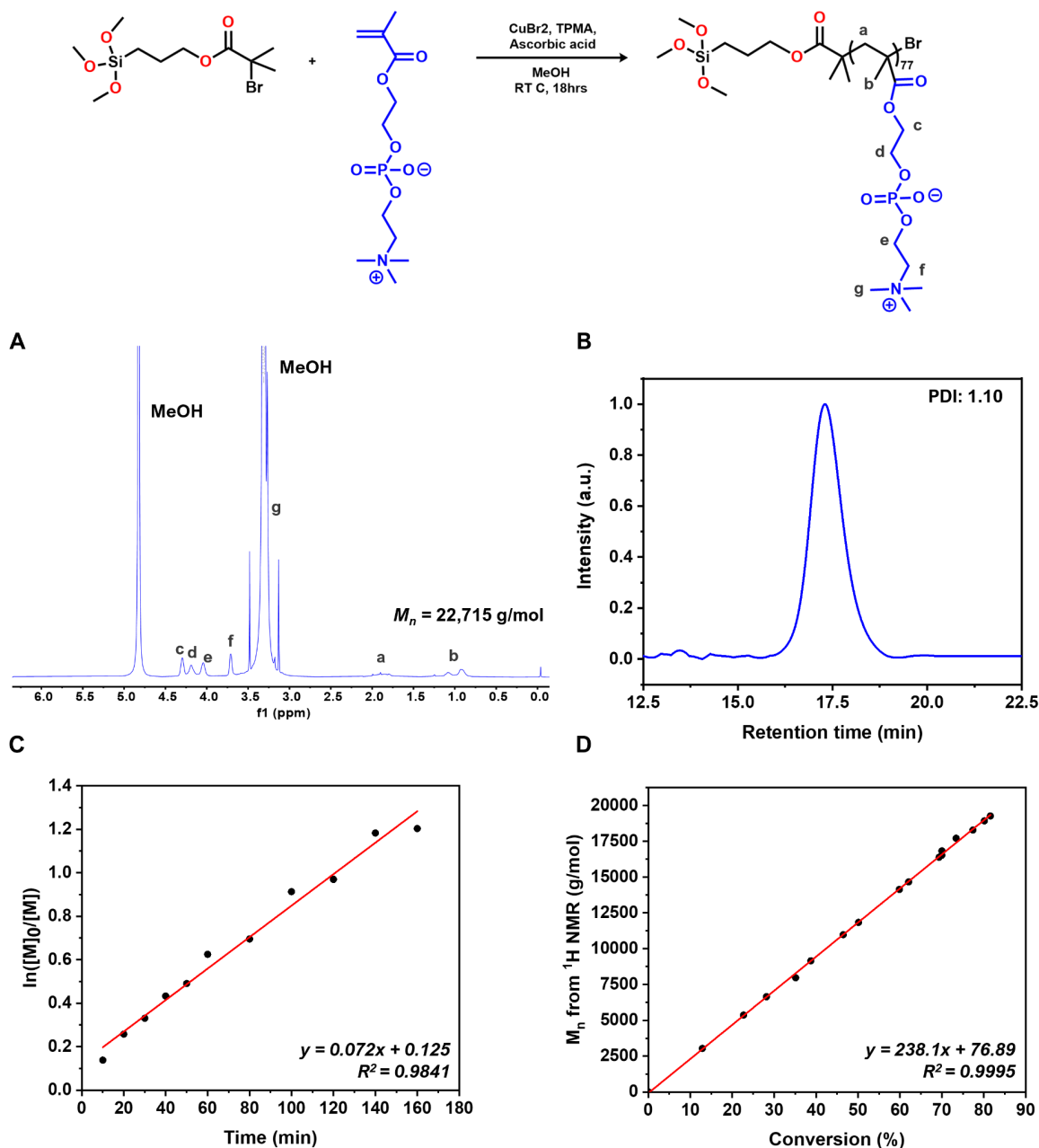


Fig. S1. Solution-polymerization of MPC using (3-trimethoxysilyl)propyl 2-bromo-2-methylpropionate as the initiator. **(A)** NMR data for final product after 18 h of reaction. **(B)** SEC of the free polymer in solution after 18 h in TFE. **(C, D)** Kinetic plots for the ARGET ATRP of MPC conducted under the same conditions as those reported in the manuscript, exhibiting the behavior characteristic of a controlled polymerization.

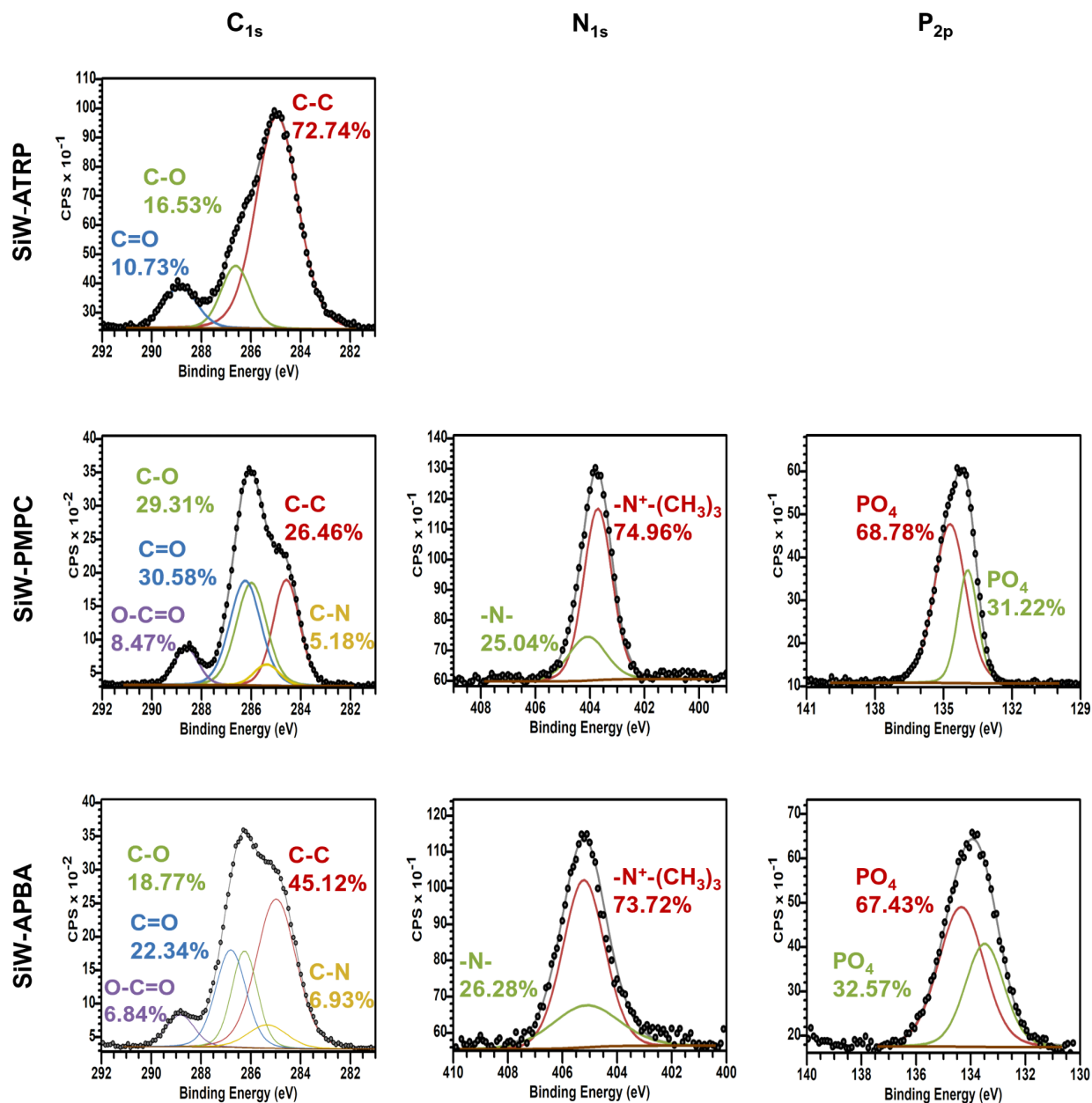


Fig. S2. High resolution XPS spectra of C_{1s}, N_{1s}, and P_{2p} peaks of -ATRP (top), -PMPC (middle) and -APBA (bottom) silicon wafers. The black dots represent experimental data and the solid gray line corresponds to the fitted data.

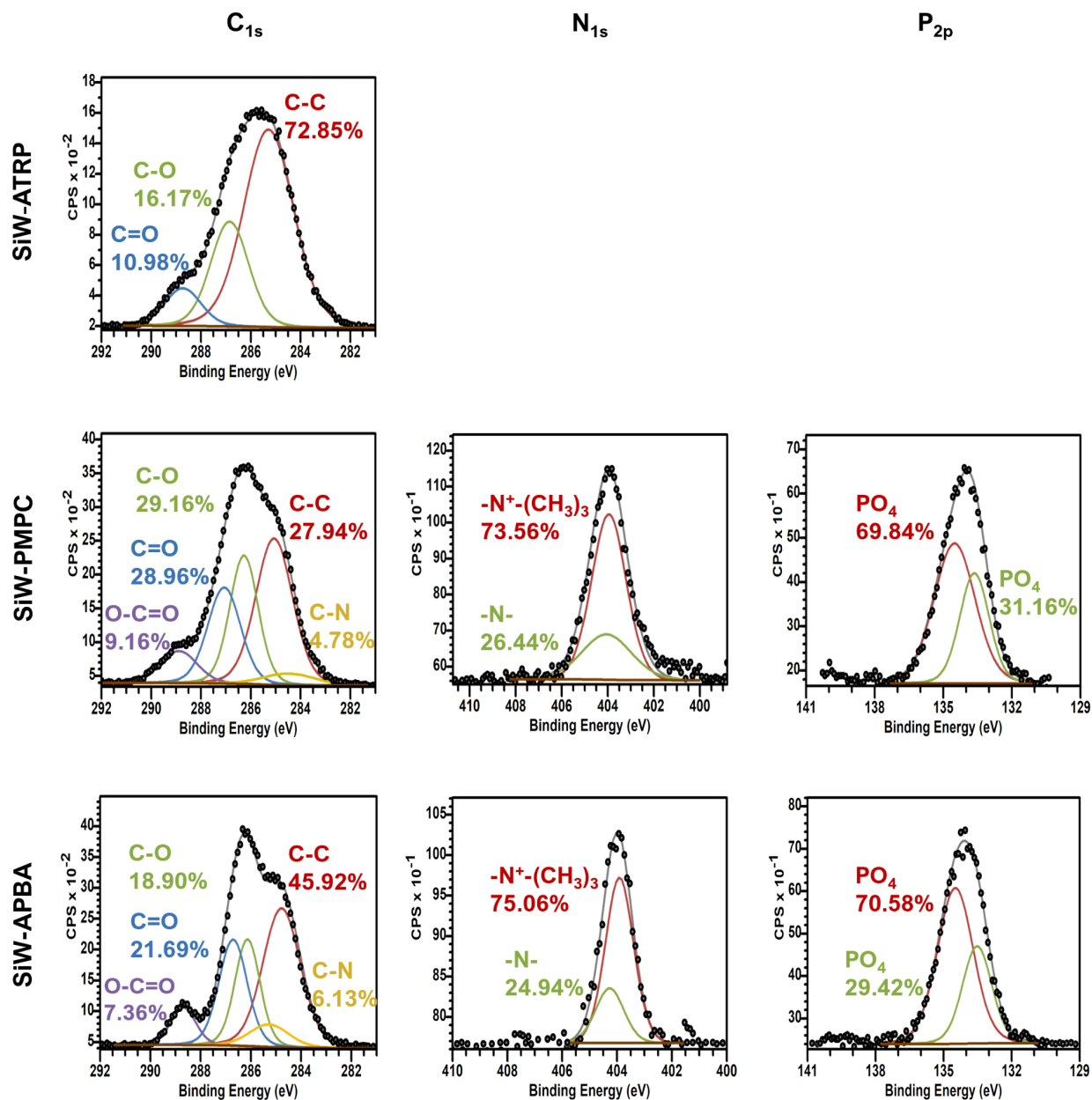


Fig. S3. High resolution XPS spectra of C_{1s}, N_{1s}, and P_{2p} peaks of –ATRP (top), –PMPC (middle) and –APBA (bottom) silica nanoparticles. The black dots represent experimental data and the solid gray line corresponds to the fitted data.

Table S1. Elemental surface composition of silica nanoparticles with different surface chemistries, obtained by XPS.

Sample	B_{1s}	C_{1s}	N_{1s}	O_{1s}	Si_{2p}	P_{2p}	Br_{3d}	N/P ratio
SiNP–Br	–	48.36	8.74	20.63	13.79	–	8.48	–
SiNP–PMPC	–	59.23	5.69	29.44	–	5.12	0.52	1.08
SiNP–APBA	0.29	59.46	5.77	29.28	–	5.20	–	1.11

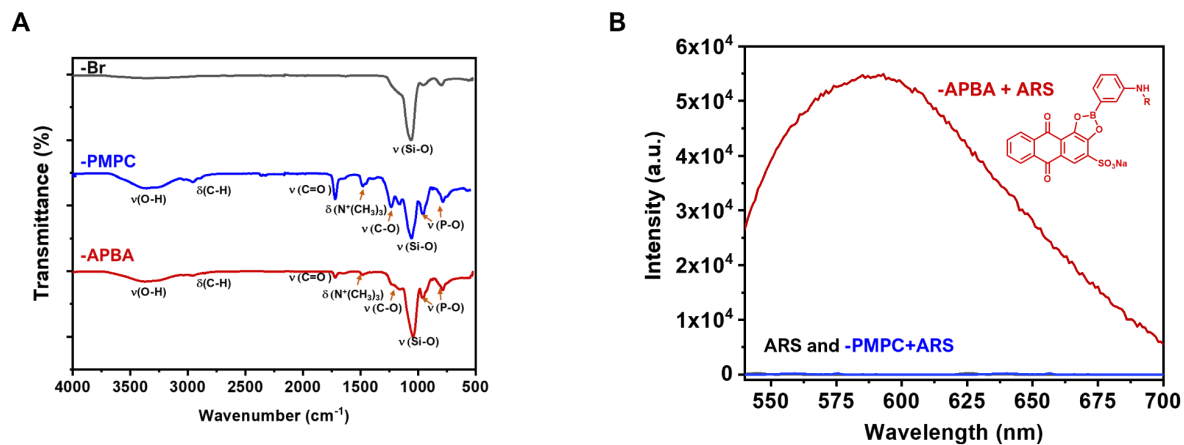


Fig. S4. Characterization of surface modified silica nanoparticles. **(A)** FTIR spectra of -Br (black), -PMPC (blue), and -APBA (red) samples showing characteristic vibrations of functional groups present in each. **(B)** Fluorescence emission spectra of -PMPC and -APBA samples demonstrating the appearance of a fluorescent species only after conjugation of ARS with the boronic acid.

Analysis of light scattering data

Dynamic light scattering (DLS) measures the change in light scattering intensity due to the Brownian motion of particles in a solution and relates it to particle size. As particles move, they scatter light at different intensities over time, and this fluctuation can be analyzed to determine particle size.

The diffusion coefficient (D) is obtained from the time correlation function, which reflects the speed at which the particles move in the solvent. Then, the hydrodynamic diameter (D_h) is related to the diffusion coefficient through the Stokes-Einstein equation as: $D_h = k_B T / 3D$

From this equation, it is determined that the diffusion coefficient is inversely proportional to the hydrodynamic diameter. Therefore, larger particles diffuse more slowly (smaller D), while smaller particles diffuse faster (larger D).^[1]

From this perspective, we focused our analysis for **Fig. 6** on the change in hydrodynamic diameter due to changes in particle diffusion caused by the interaction with mucin in the medium.

Particle random Brownian motion causes a fluctuation in the intensity of scattered light as a function of time. The correlator then constructs a correlation function (G) of the scattered intensity, which is an exponential decaying function.^[2] For a monodisperse sample, the correlation function is: $G(\tau) = A[1 + B \exp(-2\Gamma\tau)]$

Where τ is the time difference of the correlator, A is the baseline, and B is the intercept of the correlation function. Additionally, $\Gamma = Dq^2$, where D is the translational diffusion coefficient and $q = (4\pi n/\lambda_o) \sin(\theta/2)$ where n is the refractive index of the dispersant, λ_o is the laser wavelength and θ the scattering angle.

For polydisperse samples, the equation for the correlation function includes the sum of all exponential decays $g_1(\tau)$, then we can write: $G(\tau) = A[1 + Bg_1(\tau)^2]$

The correlation functions and the corresponding DLS curves of SiNP-APBA at different pH values and different sialic acid: end group ratios are presented in **Fig. S6**. Particle size is obtained from the correlation function by fitting an exponential to it so as to obtain the z-average diameter and estimate the polydispersity. The plot obtained is the relative intensity of light scattered by particles and represented as the intensity size distribution.

[1] F. Babick, In Micro and Nano Technologies: Characterization of Nanoparticles, Chapter 3.2.1 - Dynamic light scattering (DLS), *Elsevier*, 2020, 137–172

[2] E. Sutherland, S.M. Mercer, M. Everist and D.G. Leaist, *J. Chem. Eng. Data*, 2009, 54, 2, 272–278

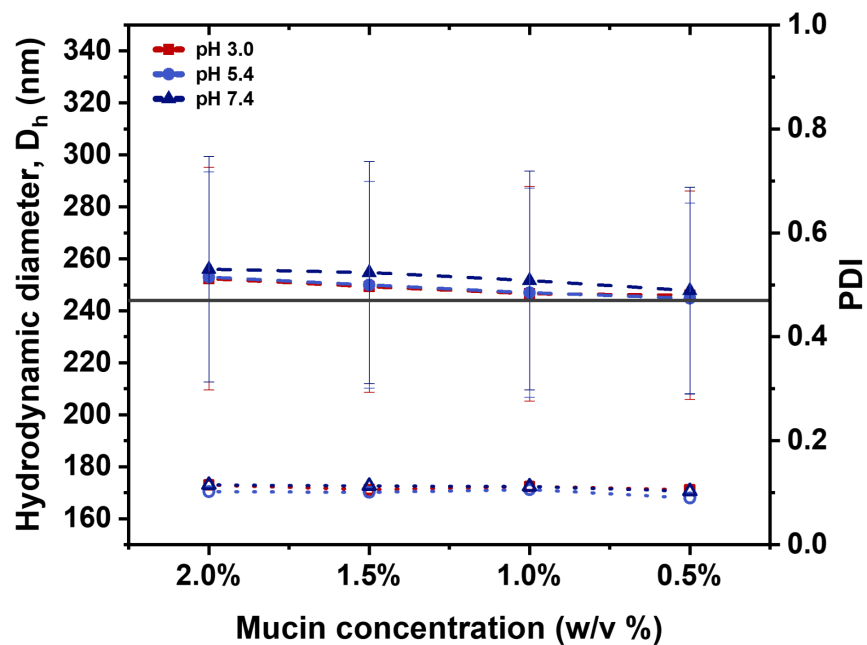


Fig. S5. Hydrodynamic diameter and polydispersity of SiNP-PMPC samples at different mucin concentrations and pH values at a SA:EG ratio of 1:1. The solid horizontal dark gray line represents the original dimensions of the particles in DI water (i.e., prior to incubation).

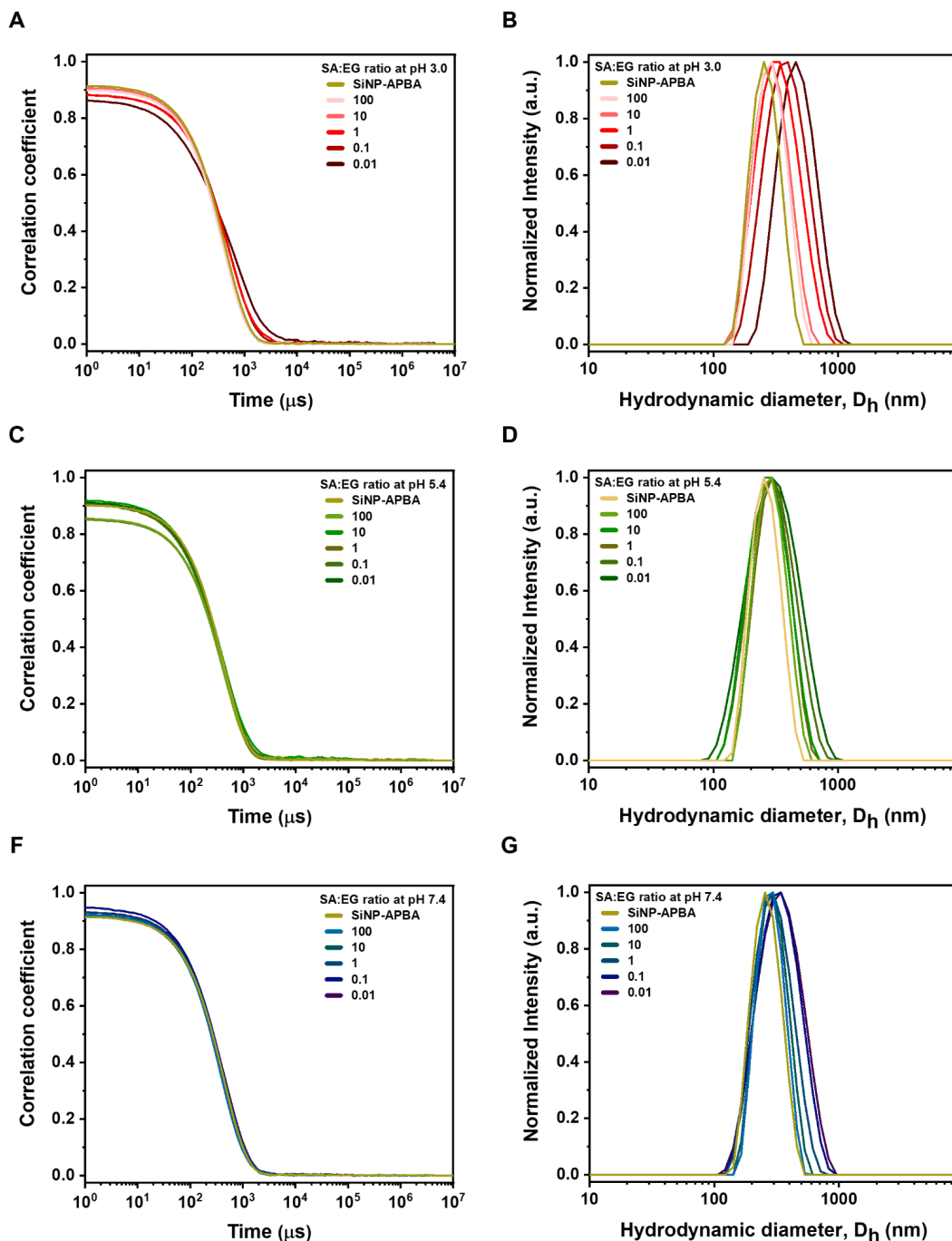


Fig. S6. Dynamic light scattering data of SiNP-APBA samples for different sialic acid: end group (SA:EG) ratios, and at pH 3.0 (A, B), 5.4 (C, D), and 7.4 (F, G). The shape of the correlation functions confirm the unimodal distribution of their corresponding hydrodynamic diameter curves. Moreover, the slower decay of the correlation function observed at pH 3.0 with decreasing SA:EG ratio confirms an increasingly more favorable interaction between mucin and the nanoparticle surface.